Isogeometric FEM-BEM coupling for magnetostatic problems modelling using magnetic scalar potential

Maxime Fays, Olivier Chadebec, Brahim Ramdane

Isogeometric FEM-BEM coupling for magnetostatic problems modelling using magnetic scalar potential

Maxime Fays[1], Olivier Chadebec[1], Brahim Ramdane[1]
[1]Univ. Grenoble Alpes, CNRS, Grenoble INP, G2Elab, 38000 Grenoble, France

The main advantage of isogeometric analysis resides in its ability to represent exactly a wide range of geometries, and has proven great efficiency in mechanical problems compared to standard finite elements. The application of the isogeometric context to electromagnetic problems leads to the isogeometric representation of air region, a particularly ineffective process. To overcome this hindrance, in a magnetostatic context, an original magnetic scalar potential Finite element - Boundary element coupling is presented. Numerical considerations and implementation specificities are discussed, and the efficiency of the method is demonstrated.

***Index Terms*—FEM-BEM, isogeometric analysis, scalar potential, magnetostatics.**

I. Introduction

THE finite element method (FEM) is widely used to study low frequency electromagnetic devices. However, it is well known that this method has a number of limitations due to its dependence on the mesh. When modeling electrical machines for instance, the accuracy of the solution in the airgap is a key point and is extremely sensitive to the accuracy of the discretization used for its description. In 2005, Isogeometric Analysis (IGA) was introduced [1], originating from the mechanical simulation community. Since its implementation, IGA has gained increasing interest over the past two decades. This method uses generalized Bézier curves, generated by a basis of spline functions, to exactly model complex geometries. The mathematical properties of the spline basis makes it a suitable choice for standard FEM projection functions, and allows to naturally embed the geometry it describes. The support of the elements of the spline basis provides parametric elements that can be used as a mesh during the assembly process, making it very similar to standard FEM assembly. In addition, having a generalized spline basis as projection and interpolation function offers great flexibility as regularity can be locally imposed, and spline orders can be elevated easily. Isogeometric analysis has proven great efficiency in standard FEM for a wide variety of problems (contact mechanics, fluid mechanics, wave propagation...) as presented in the review [2].

However, when modeling electromagnetic problems, the conventional IGA and FEM based models need a full domain representation including active (magnetic and/or conductive) regions and inactive (air) ones. As a result, the number of degrees of freedom (DoFs) can be huge. Moreover, IGA does not provide an efficient way to represent inactive regions since the air region often has a complex topology.
In order to overcome this drawback, and inspired by the FEM-BEM coupling already developed in [5], a coupling between the IGA-FEM and the boundary element method (IGA-BEM) can be developed. The IGA-BEM is used to model only the linear unbounded regions (air domain) and the IGA-FEM is used to model the non-linear active regions, allowing to benefit from both methods. In this context, as the geometry is represented exactly, a better precision per degree of freedom is expected as the only source of error is the interpolation of the solution by the shape functions. IGA-FEM-BEM coupling started developing in 2014, in mechanics [3], with only few contributions to magnetostatics except very recently in [4].
We will first introduce the basics of isogeometric analysis, then we will introduce the proposed isogeometric FEM-BEM coupling, based on the magnetic scalar potential formulation for 2D and 3D magnetostatic problems, and discuss the isogeometric specificities tied to the numerical implementation. Finally, numerical validation and results will be presented to assess the efficiency of the proposed formulation.

II. Isogeometric Analysis

A. NURBS

Non-Uniform Rational B-spline (NURBS) curves are generated as a sum of n rational basis functions $(R_{i,p})_{,\, i=1,..,n}$, of degree p, and n control points P_i:

$$C(\xi) = \sum_{i=1}^{n} R_{i,p}(\xi)\mathbf{P}_i. \tag{1}$$

The rational basis functions are constructed as a rational sum of weighted elements of a spline basis $w_j(N_{j,p})_{j=1,..,n}$:

$$R_{i,p}(\xi) = \frac{N_{i,p}(\xi)w_i}{\sum_{j=1}^{n} N_{j,p}(\xi)w_j}. \tag{2}$$

The n elements of the spline basis functions of degree p, $(N_{j,p})_{j=1,..,n}$ are constructed according to the Cox-deBoor recurrence formulae as described in [2], and the associated knot vector will be denoted $\Xi = [\xi_1, ..., \xi_m]$. Most CAD software provides default values for knot vectors, control points, and weights to create spline basis functions, which then generate the rational basis and NURBS curve. The modeling process involves altering these default values to change the shape of the default model, as shown in Figure 1. NURBS surfaces and volumes can be made by combining NURBS curves or surfaces through tensor products, and multiple NURBS elements can be used to create a single model (multipatch geometry) if needed.

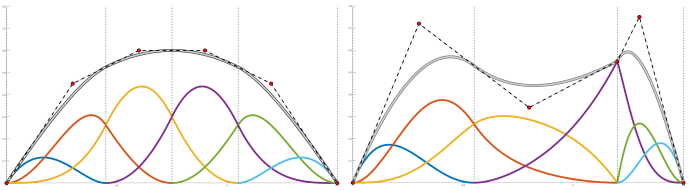

Fig. 1. **Left:** Default NURBS curve (grey), the associated control points (red) and rational basis **Right:** A modification of the default NURBS curve through knot vector, and control point modification, and the corresponding rational basis.

B. NURBS integration in conventional FEM assembly

To detail the IGA-FEM assembly process, we first introduce the parametrisations required to integrate functions over the domain Ω. The application:

$$C: \begin{cases} [0,1] \longrightarrow \Omega \\ \xi \longmapsto C(\xi) \end{cases}$$

is a parametrisation from the parametric domain to the physical domain Ω. The images of the elements $\{[\xi_i, \xi_{i+1}],\ i \in [\![1, m-1]\!]\}$, extracted from the knot vector Ξ define a cartesian grid in the parametric domain. Therefore, C can be decomposed as $C = \sum_{i=1}^{m-1} C_i$ with:

$$C_i: \begin{cases} [\xi_i, \xi_{i+1}] \longrightarrow \Omega_i \subset \Omega \\ \xi \longmapsto C(\xi). \end{cases}$$

The images of the applications C_i define a structured grid on the physical domain $\Omega = \bigcup_{i=1}^{m-1} \Omega_i$, playing the role of the mesh in standard FEM. For convenience, an extra parametrisation is used to work on a reference domain (parent space):

$$\hat{C}_i: \begin{cases} [0,1] \longrightarrow [\xi_i, \xi_{i+1}] \\ \hat{\xi} \longmapsto \xi. \end{cases}$$

Denoting J_C the Jacobian of C, the integration can be decomposed:

$$\begin{aligned} \int_\Omega f(x)d\Omega &= \int_{[0,1]} f(C(\xi))|\mathrm{J}_C(\xi)|d\xi \\ &= \sum_{i=1}^{m-1} \int_{[0,1]} f(C_i \circ \hat{C}_i(\hat{\xi}))|\mathrm{J}_{C_i \circ \hat{C}_i}(\hat{\xi})|d\hat{\xi} \end{aligned} \tag{3}$$

which can be evaluated using usual integration routines. This process can be generalized to higher dimensions (surfaces/volumes) and to multipatch geometries. Figure 2 illustrates the different parametrisations on a simple 2D case.

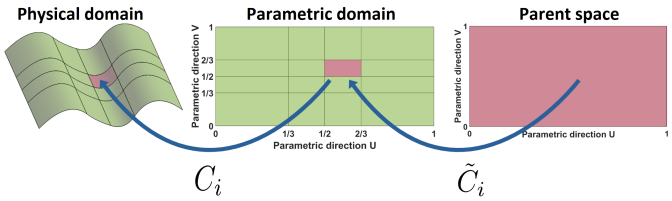

Fig. 2. Illustration of the different parametrisations involved when integrating a quantity on the physical domain

In addition, the standard FEM shape functions are replaced by the rational basis $(R_{i,p})_{,\ i=1,\dots,n}$ that generated the geometry, the unknown are placed at control points and equation (1) allows the reconstruction of the solution directly on the modeled domain. Although the structured grid and the rational basis are imposed by the geometry, they can be modified: refining the structured grid (h-refinement), increasing the order of the spline basis (p-refinement) and local modification of the continuity of the spline basis are all managed by knot vector modifications (mostly insertion of elements) without re-modeling nor geometry modification, giving the shape functions more flexibility than in standard FEM throughout the resolution process.

III. Isogeometric FEM-BEM coupling

A. Formulation

In this work, we are interested in the solving of magnetostatic problems. The studied domain is decomposed into non linear magnetic materials Ω_{Active} region with boundary Γ_{Active} and an air region Ω_{Air} containing static currents which create a source magnetic field $\mathbf{H_s}$. In order to develop our isogeometric FEM-BEM approach, a H-conforming formulation is chosen with magnetic scalar potentials as state variables as opposed to [4], where a vector potential is used. This choice is explained by the handling of scalar degrees of freedom which are easier to treat in the IGA context, and the absence of gauge. In addition, an integration strategy is proposed to integrate strongly singular integrals, and allow 3D problems.
Due to the so-called cancellation error problem, using a reduced potential in the active domain would lead to numerical instabilities for magnetic materials with high permeabilities, worsened when considering non-linear materials, a coupled total-reduced scalar potential decomposition of $\mathbf{H}$ is preferred [5]. It should be noticed here that this formulation is known to pose problems with multiply connected magnetic regions. Magnetic cuts can probably be used to address this issue, as standard mesh based algorithm would still work on the structured grid. For a given magnetic source field $\mathbf{H_s}$, we decompose the magnetic field $\mathbf{H}$:

$$\begin{aligned} \mathbf{H} &= -\nabla\phi \quad \text{in } \Omega_{\text{Active}} \\ \mathbf{H} &= \mathbf{H_s} - \nabla\phi_r \quad \text{in } \Omega_{\text{Air}} \end{aligned} \tag{4}$$

and solve:

$$-\mathrm{div}(\mu\nabla\phi) = 0 \text{ in } \Omega_{\text{Active}} \tag{5}$$

$$\Delta\phi_r = 0 \text{ in } \Omega_{\text{Air}} \tag{6}$$

with interface conditions:

$$\mathbf{n} \times (\mathbf{H_{active}} - \mathbf{H_{air}}) = 0 \qquad \text{on } \Gamma_{\text{Active}} \tag{7}$$

$$\mathbf{n} \cdot (\mathbf{B_{active}} - \mathbf{B_{air}}) = 0 \qquad \text{on } \Gamma_{\text{Active}} \tag{8}$$

Firstly, denoting $Tu = u_{|\Gamma}$ the trace operator on the boundary Γ, and remarking that $\nabla_{|\Gamma} = \mathbf{n} \times \nabla$ on Γ, (7) can be written:

$$\mathbf{n} \times (\nabla(\phi_r - \phi)) = \mathbf{n} \times \mathbf{H_s} \tag{9}$$

$$\nabla_{|\Gamma}(\phi_r - \phi) = \mathbf{n} \times \mathbf{H_s} \tag{10}$$

which projected on test functions $\nabla w_{i|\Gamma}$ leads to the weak form:

$$\int_{\Gamma_{\text{active}}} \nabla w_{i|\Gamma} \cdot \nabla_{|\Gamma}(\phi_r - \phi) = \int_{\Gamma_{\text{active}}} \mathbf{H_s} \nabla w_{i|\Gamma}. \tag{11}$$

Pre-solving this equation gives a solution $\delta\phi = \phi_r - \phi$ allowing to express the reduced potential with the total one: $\phi_r = \phi + \delta\phi$ on the interface Γ_{Active}.
This simple finite element pre-resolution forces the construction of a trace space, which is easy to build if the NURBS surface/volume geometry was constructed as a tensor product of NURBS curves/surfaces, as the rational basis on the boundary can be canonically recovered.
In Ω_{Active}, equation (5) is treated with an isogeometric finite element method. Denoting B_n the normal component of $\mathbf{B}$, doing an integration by part, using the divergence theorem and imposing strongly (8) yields:

$$\int_{\Omega_{\text{active}}} \nabla w_i \cdot \mu \nabla \phi = -\int_{\Gamma_{\text{active}}} w_i \mathrm{B}_n. \tag{12}$$

In Ω_{Air}, equation (6) is computed with an isogeometric boundary element method. Using Green's third identity, with:

$$G(x,y) = \frac{1}{2\pi}\ln(r), \text{ with } r = ||x-y|| \quad \text{for } x,y \in \mathbb{R}^2 \tag{13}$$

$$G(x,y) = -\frac{1}{4\pi r}, \text{ with } r = ||x-y|| \quad \text{for } x,y \in \mathbb{R}^3 \tag{14}$$

we can write the boundary integrals:

$$\begin{aligned}\int_{\Gamma_{\text{active}}} w_{i|\Gamma} \frac{\phi+\delta\phi}{2} = &-\int_{\Gamma_{\text{active}}} w_{i|\Gamma} \int_{\Gamma_{\text{active}}} \frac{dG}{dn}(\phi+\delta\phi) \\ &+ \int_{\Gamma_{\text{active}}} w_{i|\Gamma} \int_{\Gamma_{\text{active}}} G(-\frac{\mathrm{B}_n}{\mu_0} + \mathrm{H}_{\mathrm{s_n}}).\end{aligned} \tag{15}$$

Equations (12) and (15) are then coupled through B_n, and the global matrix system can be written:

$$\left(\begin{array}{c|c} \mathbf{FE1} & \begin{array}{c}0\\ \hline \mathbf{FE2}\end{array} \\ \hline 0 \;|\; \mu_0\mathbf{K} & \mathbf{T} \end{array}\right) \left(\begin{array}{c}\phi \\ \mathrm{B_n}\end{array}\right) = \left(\begin{array}{c}0 \\ \mathbf{R}\end{array}\right)$$

Where:

$$\mathbf{FE2} = \int_{\Gamma_{\text{active}}} w_{i|\Gamma} w_{j|\Gamma}, \quad \mathbf{K} = \frac{\mathbf{FE2}}{2} + \int_{\Gamma_{\text{active}}} w_{i|\Gamma} \int_{\Gamma_{\text{active}}} \frac{dG}{dn} w_{j|\Gamma}$$

$$\mathbf{FE1} = \int_{\Omega_{\text{active}}} \nabla w_i \cdot \mu \nabla w_j, \quad \mathbf{T} = \int_{\Gamma_{\text{active}}} w_{i|\Gamma} \int_{\Gamma_{\text{active}}} G w_{j|\Gamma}$$

$$\mathbf{R} = \int_{\Gamma_{\text{active}}} w_{i|\Gamma} \int_{\Gamma_{\text{active}}} G\mathrm{H}_{\mathrm{s_n}} - \mathbf{K}\delta\phi$$

The shape functions to approximate ϕ are numbered in such a way that the ones not vanishing at the boundary are placed at the end, giving the zero blocks correspondence to functions vanishing on the boundary. The reconstruction of $\mathbf{H}$ in Ω_{Air} is done in post-processing:

$$\mathbf{H} = \mathbf{H_s} + \int_{\Gamma_{\text{active}}} \nabla \frac{dG}{dn}(\phi+\delta\phi) - \int_{\Gamma_{\text{active}}} \nabla G(-\frac{\mathrm{B}_n}{\mu_0} + \mathrm{H}_{\mathrm{s_n}}) \tag{16}$$

To consider non-linear permeability, we apply the Newton–Raphson technique. Although it involves the evaluation of every matrix, only the derivative of the finite element part

$$\int_\Omega \nabla w_i \mu[\mathbf{H}] \nabla w_j$$

is required, and the procedure is as fast as in standard FEM-BEM couplings.

B. Isogeometric assembly process

The IGA assembly process has some implementation specifics and requires some numerical considerations. The assembly process is generally more complex than the standard FEM-BEM assembly [7].
The assembly process is more efficient when the structure of the surfaces/volumes generated through tensor products is maintained, as it allows only the parametric directions to be considered instead of the entire surface. This results in a matrix assembly being performed for each parametric direction, with flexible shape functions as illustrated in Figure 1 (varying support, continuity, value, ...). Furthermore, it is common to work with multipatch geometries, where a structure must be created for each individual geometry and a global structure must also be established, which connects the degree of freedom at the interfaces between patches and assigns a global numbering for the degree of freedom. For the presented coupling, a multipatch geometry structure is generated for the domain Ω_{Active} and for the boundary domain Γ_{Active} as shown in Figure 3, such that the B-spline in Γ_{Active} are the traces of the B-spline of Ω_{Active}. In particular, it is important to be able to link

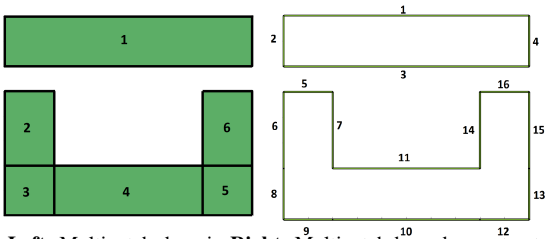

Fig. 3. **Left:** Multipatch domain **Right:** Multipatch boundary extracted from the multipatch domain

every boundary DoFs of Ω_{Active} to their corresponding DoFs in Γ_{Active} as they are coupled through the matrices **FE1**,**K**, and the pre-resolution.
Moreover, the singularities of the boundary element integrals in $\mathbf{K}$ and $\mathbf{T}$ are computed with a Telles transform [6]. The Telles transform aggregates the target Gauss points towards the source points through a polynomial transformation, and provides a Gauss point efficient mean of computing singular integrals.
Suppose we want to integrate $\int_{-1}^{1} f(x)dx$, with a singularity $\bar{x} \in [0,1]$, using a Gauss-Legendre quadrature. We define:

$$\bar{\gamma} = \sqrt[3]{\bar{x}(\bar{x}^2-1) + |(\bar{x}^2-1)|} + \sqrt[3]{\bar{x}(\bar{x}^2-1) - |(\bar{x}^2-1)|} + \bar{x} \tag{17}$$

And we integrate:

$$\int_{-1}^{1} f[\frac{(\gamma-\bar{\gamma})^3 + \bar{\gamma}(\bar{\gamma}^2+3)}{(1+3\bar{\gamma})^2}] \frac{3(\gamma-\bar{\gamma}^2)}{(1+3\bar{\gamma})^2} dx. \tag{18}$$

As the polynomial transformation is known for every source point, and only consists in a change of variable, it can be encoded in a quadrature rule, and the necessary structures can be generated before assembling the dense matrices. Figure 4 illustrates the new quadrature obtained after a Telles transform on a standard Gauss-Legendre quadrature.
In addition, standard matrix compression techniques can be used to handle the dense BEM matrices.

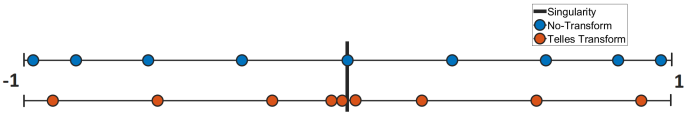

Fig. 4. Distribution of a Gaussian quadrature (9 points) on [-1,1] before, and after applying the Telles Transform, to compute a singular integral with a singularity located in $\bar{x} = 0$.

IV. Validation and Results

The validation of the developed model has been carried out first on a 2D simple academic case consisting in a magnetic disk in a uniform magnetic field $\mathbf{H_S}$, where the analytical solution is known. Figure 5 illustrates the structured grid after two differrent h-refinement levels on the geometry, to increase the number of degrees of freedom, and the solution $\nabla\phi$ at the finest level. Figure 6 shows the relative error comparison

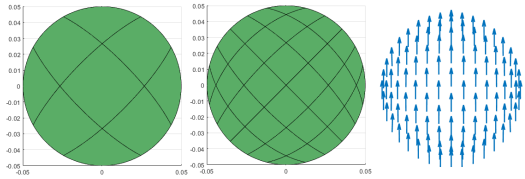

Fig. 5. Successive h-refinement on the geometry, and the computed potential $\nabla\phi$ on the finest structured grid.

of $\nabla\phi$ and B_n to the reference solution for different levels of h-refinement. It should be noticed that a good accuracy is obtained using only a few DoFs, and that the geometry only needs to be imported once. To illustrate the flexibility offered

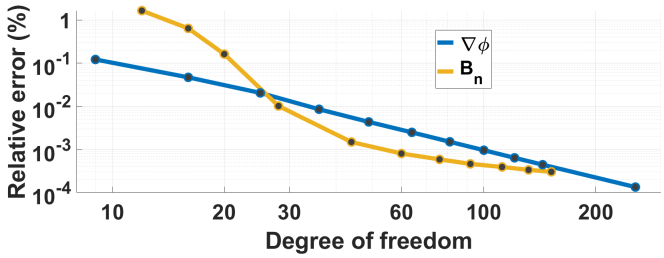

Fig. 6. Relative error comparison of $\nabla\phi$ and B_n obtained using the presented IGA-FEM-BEM coupling to a reference solution.

by Isogeometric Analysis, we can transform the geometry of Figure 5 into a square, via weight modifications, and re-compute the solution with different levels of h-refinements on the new geometry. The developed method has then been used

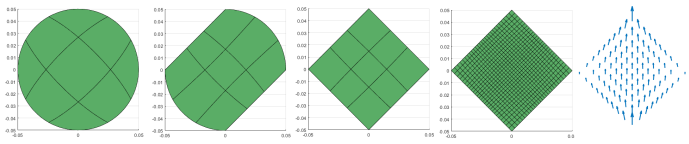

Fig. 7. Successive transformation of the initial geometry, followed by h-refinement, and the computed potential $\nabla\phi$

to model a 2-dimensional actuator. It is a magnetic circuit with a coil as shown in Fig.8(a). In order to handle the geometry, the active domain is decomposed into multiple NURBS patches. The Figure 8(b) illustrates the magnetic field cartography.

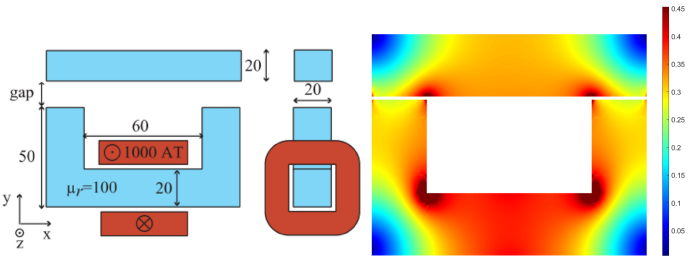

Fig. 8. a) scheme of the modeled Actuator. b) Norm of the magnetic field B inside the actuator generated with multiple NURBS patches.

The presented coupling is not restricted to 2D models, and to demonstrate the geometric descriptive ability of NURBS, we have modeled a 3-dimensional actuator, with a circular core. The results presented in Figure 9 are in good agreement with the expected physical solution, with few DoFs ($\approx$ 750) compared to the conventional FEM-BEM.

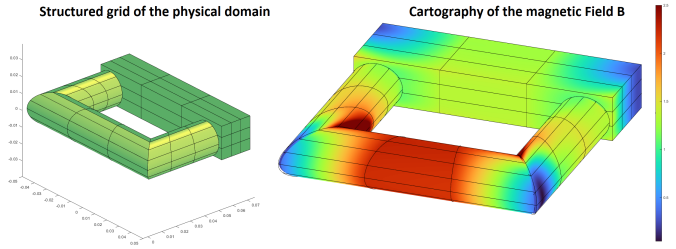

Fig. 9. Cartography of the magnetic field B on a 3-dimensional circular core actuator with only 740 DoFs

V. Conclusion

In this work, a new IGA-FEM-BEM formulation based on the magnetic scalar potential has been developed to model magnetostatic problems. The key points of the method have been discussed and addressed. The presented Isogeometric FEM-BEM coupling allows a good geometric descriptive ability and an easy geometry access. In addition, the approach maintains a typical FEM-BEM precision with fewer required DoFs.

References

[1] T.J. Hughes, J.A. Cottrell, Y. Bazilevs, "Isogeometric analysis: CAD, finite elements, NURBS, exact geometry and mesh refinemen", Computer methods in applied mechanics and engineering, 2005 vol. 194(39-41), p. 4135-4195.

[2] V.P. Nguyen, C. Anitescu, S.P. Bordas, T. Rabczuk, "Isogeometric analysis: an overview and computer implementation aspects", Mathematics and Computers in Simulation, 2015, vol. 117, p. 89-116.

[3] S. May, M. Kästner, S. Müller, V.Ulbricht, "A hybrid IGAFEM/IGABEM formulation for two-dimensional stationary magnetic and magneto-mechanical field problems", Computer Methods in Applied Mechanics and Engineering, 2014, vol. 273, p. 161-180.

[4] M. Elasmi, C. Erath, S. Kurz, "Non-symmetric isogeometric FEM-BEM couplings", Advances in Computational Mathematics, 2021, 47(5), p. 1-36.

[5] I. Mayergoyz, M. Chari, J. D'angelo, "A new scalar potential formulation for three-dimensional magnetostatic problems", IEEE transactions on magnetics 1987, 23(6), 3889-3894.

[6] J. Telles, "A self-adaptive co-ordinate transformation for efficient numerical evaluation of general boundary element integrals", International journal for numerical methods in engineering, 1987 24(5), 959-973.

[7] C. De Falco, A. Reali, R. Vázquez, "GeoPDEs: a research tool for isogeometric analysis of PDEs", Advances in Engineering Software, 2011, 42(12), 1020-1034.